Journal of Non-Crystalline Solids 320 (2003) 9–20

Glass-forming ability versus stability of silicate glasses. II. Theoretical demonstration

I. Avramov [1], E.D. Zanotto [*], M.O. Prado [2]

Vitreous Materials Laboratory (LaMaV), Department of Materials Engineering (DEMa), Federal University of São Carlos (UFSCar) 13565-905, São Carlos-SP, Brazil

Received 19 June 2002

Abstract

Possible relationships between measures of glass stability (GS) against devitrification on heating (evaluated by the Hrubÿ parameter $K_H = (T_c^h - T_g)/(T_m - T_c^h)$, and the parameter $K_w = (T_c^h - T_g)/T_m$) and a criterion of glass-forming ability (GFA) – the critical cooling rate – were investigated by computing non-isothermal crystallization for typical values of the main quantities that control crystal nucleation and growth in silicate glasses. We limit these quantities to one thermodynamic parameter – the melting entropy (ΔS_m) and two kinetic parameters that control the viscosity (B and T_0 in the Vogel–Fulcher–Tamman equation or T_g and α in Avramov's equation). The effect of heterogeneous nucleation and, in particular, the possible role of the surface as active substrate is tested. The results presented herein demonstrate that GS and GFA are indeed related concepts.
© 2003 Elsevier Science B.V. All rights reserved.

1. Introduction

The ability of substances to vitrify on cooling from the melt is known as glass-forming ability (GFA) and has been the object of theoretical and experimental investigations for several decades. Both structural (or microscopic) and kinetic (or phenomenological) methods have been proposed to understand GFA.

The first structural methods were proposed in the 1920s. In 1926, for instance, Goldschmidt [1] assumed that glass-forming substances have a ratio of cation radius, r_c, to anion radius, r_a, within $0.2 < r_c/r_a < 0.4$. Although all ionic glass-formers satisfy this rule, there are many systems that satisfy it but are not glass-formers (e.g., BeO and most of the halides). In 1932, Zachariasen [2] formulated the well-known random network theory, according to which glass-formers are cations that have high valences ($\geqslant 3$) and can create three-dimensional networks of polyhedra, which interconnect by corners and not by edges or faces. In the case of silicate, germanate, borate and phosphate glasses, oxygen networks are formed by polymerization of

[*] Corresponding author. Tel.: +55-16 271 4871; fax: +55-16 261 5404.

E-mail addresses: avramov@ipc.bas.bg (I. Avramov), dedz@power.ufscar.br (E.D. Zanotto).

[1] On leave from the Institute of Physical Chemistry, Bulgarian Academy of Sciences, 1113 Sofia, Bulgaria.

[2] On leave from the Comisión Nacional de Energía Atómica, Centro Atómico Bariloche, 8400-S.C. de Bariloche, Argentina.

0022-3093/03/$ - see front matter © 2003 Elsevier Science B.V. All rights reserved.
doi:10.1016/S0022-3093(03)00081-4

polyhedra. Several other structural approaches have been proposed along the last few decades. Structural approaches, however, do not take the thermal history of the melt into account.

Tamman [3] introduced kinetic concepts in 1922. He assumed that glasses are formed when the nucleation rate versus temperature curve, $J(T)$, does not significantly overlap the growth rate $G(T)$ curve. Later on, in 1956, Dietzel and Wiekert [4] considered stability against crystallization and how this depends on the crystal growth rate. Turnbull and Cohen [5] proposed the determination of kinetic stability on cooling experiments through the steady-state nucleation rate in 1960. In fact, their approach implies an infinitely fast growth rate (which is valid for liquid metals, for instance). More recently, Gutzow et al. [6] related glass stability (GS) to the non-steady-state time lag, τ. All these kinetic approaches assume that one of the three parameters (J, G or τ) is dominant and neglect the other two.

In 1972, Uhlmann et al. [7] took J and G into account simultaneously, formulating a kinetic criterion for vitrification. They later extended the kinetic theory of glass formation to include non-steady state effects and heterogeneous nucleation (see, for instance, [6] and literature cited therein).

In 1989, Weinberg et al. [8,9] demonstrated that the volume fractions transformed and the resulting critical cooling rates, R_c, are quite sensitive to the method of calculation. The so-called 'nose method', for instance, which uses isothermal TTT curves, overestimates R_c by up to one order of magnitude.

In a subsequent paper [10], the same authors demonstrated that R_c are highly sensitive to the main physical properties that govern nucleation and growth kinetics: crystal liquid surface energy, thermodynamic driving force and viscosity.

Later on, in 1994, Weinberg [11] integrated the equation of overall crystallization kinetics to estimate and compare criteria for vitrification on cooling and GS against crystallization on heating. He compared the trends in computed GFA and GS ($K_w = (T_c^h - T_g)/T_m$) against melting entropy ΔS_m, and two viscosity parameters: the Kauzmann temperature, T_0, and apparent activation energy, $B[\log \eta = A + B/(T - T_0)]$. He found that both GFA and GS increased with an increase of ΔS_m and T_0; however, GFA and GS moved in *opposite* directions (decrease of GFA and increase of GS) with an increase of B (in this case, a concomitant *decrease* in the pre-exponential term A of the viscosity equation was imposed). From these results, Weinberg concluded that GFA and GS are ill-related concepts.

However, in 1997, Cabral et al. [12] used *experimental* values of crystal nucleation and growth rates for four glasses that nucleate in the bulk to calculate critical cooling rates for glass formation (R_c) by the TTT method. The resulting values of R_c were consistent with their laboratory practice of melting and quenching the studied glasses and also with experimental data of R_c for one of the glasses, lithium disilicate. They found a correlation between the Hrubÿ parameter of GS (K_H) and GFA.

Since these two last papers reached contradictory conclusions, to settle this problem we decided to check the two approaches; the theoretical calculations of Ref. [11] and the experimental data and approach of Ref. [12] through further testing. We began by repeating all the calculations of Ref. [11], using exactly the same assumptions, and confirmed his results. In this paper, therefore, we repeat and extend the calculations of Ref. [11], but test a different assumption, which is supported by experimental data, i.e., that the activation energy for viscous flow, B, varies *independently* of the pre-exponential term, A. Under this assumption, we demonstrate that GFA and GS are indeed related quantities, a finding that is corroborated by the experimental results of Cabral et al. [12].

2. Theory

GFA accounts for the easy vitrification of a melt when cooled from above the liquidus, T_m, to the glass transition, T_g, temperature. This parameter is characterized by the *critical cooling rate*, $q_{cr}(x_c)$, which is the lowest cooling rate at which the final degree of crystallinity of the frozen liquid will not exceed a given critical value, x_c, normally assumed to be within 10^{-6}–10^{-2} [7].

GS, on the other hand, accounts for the resistance of a glass towards devitrification upon re-

heating. Quantitative measurements of GS are formulated through the T_c^h temperature of the maximum crystallization rate observed in non-isothermal experiments. T_c^h is usually taken as the peak crystallization temperature determined by DSC or DTA measurements.

The most popular criteria to access GS accounts for the position of the crystallization temperature, T_c^h, which is always located between the glass transition temperature, T_g, and the melting (or liquidus) temperature, T_m.

$$K_H = \frac{T_c^h - T_g}{T_m - T_c^h}, \quad K_W = \frac{T_c^h - T_g}{T_m}. \tag{1}$$

The former parameter, K_H (the Hrubÿ parameter), and the latter, K_W, are often used to estimate GS. The larger the K_H, or K_w, the greater the stability of the glass against devitrification.

Critical cooling rates are normally rather difficult to measure; hence, it is important to assess GFA via other easily measured properties such as GS parameters, which can be readily determined via DTA or DSC.

The aim of this article is, therefore, to investigate a possible correlation between GS and GFA. We integrate numerically the equation of overall crystallization, testing the most important physical parameters that control crystallization and the way these parameters influence the degree of crystallization on both cooling and heating paths. GFA and GS are investigated in systems that undergo homogeneous and heterogeneous nucleation.

The theoretical basis for interpreting overall crystallization kinetics is given by the theory of transformation kinetics long ago proposed by Kolmogorov [13] and Avrami [14,15]. Considering the limiting case of isothermal homogeneous nucleation with simultaneous growth of spherical crystals, the crystallized fraction, x, depends on the nucleation frequency per unit volume, $J(t)$, and on the crystal growth rate, $G(t)$, expressed as

$$x = 1 - \exp\left[-\frac{4\pi}{3} \int_0^t J(t') \left(\int_{t'}^t G(\tau)\,\mathrm{d}\tau \right)^3 \mathrm{d}t' \right]. \tag{2}$$

When a system is subjected to a constant cooling (or heating) rate q,

$$q = \frac{\mathrm{d}T}{\mathrm{d}t}. \tag{3}$$

Eq. (2) transforms to

$$x(q) = 1 - \exp\left\{ -\frac{4\pi}{3q} \int_{T_m}^T J(T') \times \left[\frac{1}{q} \int_{T'}^T G(T'')\,\mathrm{d}T'' \right]^3 \mathrm{d}T' \right\}. \tag{4}$$

The critical cooling rate necessary to crystallize a fraction x_c, $q_c(x_c)$, determined from Eq. (4), is thus

$$q_{cr}(x_c) = \left[-\frac{\frac{4\pi}{3} \int_{T_m}^T J(T') \left[\int_{T'}^T G(T'')\,\mathrm{d}T'' \right]^3 \mathrm{d}T'}{\ln(1 - x_c)} \right]^{\frac{1}{4}}. \tag{5}$$

The crystal growth rate in silicate glasses is given by (see for instance [6])

$$G = W \frac{d_0}{\tau_G} \left[1 - \exp\left(-\frac{\Delta\mu}{RT} \right) \right], \tag{6}$$

where $W < 1$ is the concentration of possible growth sites on the crystal/melt interface, which depends on the growth mechanism, τ_G is the time required by the building units to cross the interface, d_0 is the mean intermolecular distance, $\Delta\mu$ is the driving force and R is the gas constant. The steady-state nucleation rate J is determined as

$$J = \frac{\Gamma}{d_0^3 \tau_J} \exp\left(-\frac{A_k}{kT} \right), \tag{7}$$

where A_k is the work of formation of a critical nucleus, Γ is the Zeldovich parameter, and τ_J is the characteristic time required to cross the melt/nucleus interface.

Voelksh [16] recently discovered that the chemical composition of cordierite nanocrystals differs from both the chemical composition of larger (microscopic) crystals and from that of the cordierite glass matrix. Fokin et al. [17] confirmed this finding in a detailed study of a soda–lime–silica glass. Although this finding is quite significant, its implications will be discussed elsewhere.

We consider here only systems in which the crystals and matrix have the same composition (single component systems), concentrating on a number of important properties that control GS and GFA. We therefore use the following assumptions:

(i) The driving force, $\Delta\mu$, is approximated through the melting entropy, ΔS_m, and temperature, T, by the Turnbull equation:

$$\Delta\mu = \Delta S_m T_m (1 - T/T_m). \tag{8}$$

This equation is valid at low undercoolings or when the specific heat of glass and isochemical crystal is similar.

(ii) The crystal/melt interface energy is expressed using the Scapski–Turnbull equation (see [5,6]):

$$\sigma \approx \alpha \frac{\Delta S_m T_m}{N_a d_0^2}, \tag{9}$$

where N_a is Avogadro's number, and α is a dimensionless constant, which should vary between $0.30 < \alpha < 0.55$ [11]. Indeed, in *fitting* the experimental temperature dependence of J for several silicate glasses, Weinberg et al. [18] found that α varies within $0.40 < \alpha < 0.5$ (under the assumption that σ is temperature and size independent). Therefore, in our calculations we assume $\alpha = 0.4$.

(iii) We assume the *screw dislocation* growth mechanism ($W \approx \frac{1-T/T_m}{4\pi\alpha}$) because it is the most typical for silicate glasses. According to Jackson, e.g., [6], normal growth is expected only for materials having a low melting entropy ($\Delta S_m < 2R$). However, it should be noted that the replacement of screw dislocation growth by normal growth does not lead to important changes in final results.

(iv) We assume that both characteristic times, τ_G and τ_J, are *equal* to the characteristic time of viscous flow, τ_η. The latter is simply related to the shear viscosity, η, by the Maxwell relation

$$\tau_\eta = \frac{\eta}{H_\infty}, \tag{10}$$

where H_∞ is the shear modulus, $H_\infty \sim 9 \times 10^{10}$ Pa for oxide glasses. An alternative expression for τ_η is given by Frenkel:

$$\tau_\eta = \frac{d_0^3 \eta}{k_B T} = \frac{V_m \eta}{RT}. \tag{11}$$

The values of τ_η obtained using Eqs. (10) and (11) are of the same order and have a similar temperature trend, which is basically defined by the viscosity.

Assumption (iv) deserves some additional comments. The (short-range) interfacial rearrangements that control crystal nucleation and growth are *not* necessarily the same as the molecular motions involved in viscous flow. There is growing evidence [19–21] that, unlike τ_η, the time τ_G is not controlled by the shear viscosity at temperatures close to T_g. To take into account the possible differences between τ_G, τ_J and τ_η is a tempting problem for future investigations. However, this possibility still needs additional experimental and theoretical verification. Therefore, in the present article, we confine ourselves to the simplest case given by assumption (iv).

2.1. Crystal growth and steady-state nucleation rate

With the above considerations, the linear growth rate G is given by

$$G = \frac{H_\infty}{4\pi\alpha\eta}\left(1 - \frac{T}{T_m}\right)\left[1 - \exp\left(-\frac{\Delta S_m}{R}\left(\frac{T_m}{T} - 1\right)\right)\right]. \tag{12}$$

Accordingly, the nucleation rate J becomes

$$J = \frac{4H_\infty}{d_0\eta\left(\frac{T_m}{T} - 1\right)}\sqrt{\frac{\alpha}{3\pi}\frac{T_m}{T}\frac{\Delta S_m}{R}\Phi}\,\exp\left(-\frac{16\alpha^3 \frac{\Delta S_m}{R}\Phi}{\frac{T}{T_m}\left(1 - \frac{T}{T_m}\right)^2}\right), \tag{13}$$

where the wetting function $0 \leqslant \Phi \leqslant 1$ accounts for the lowering of the energy of formation of a critical nucleus in heterogeneous nucleation. Because the number of nucleation sites in heterogeneous nucleation depends on many factors, such as impurities and defects, one must be aware that the pre-exponential in Eq. (13) can change for each condition. Due to the numerous possible cases, this correction has not been introduced in Eq. (13),

since we are interested mainly in trends rather than in absolute values.

2.2. Expressions for viscosity

In general, viscosity is expressed as

$$\eta = \eta_0 \exp\left(\frac{E(T)}{k_B T}\right), \tag{14}$$

where the effective value of activation energy $E(T)$ depends on temperature, while the pre-exponential constant η_0 depends on the mean vibration frequency of the building units, $\nu_0 \sim 10^{-12}$ s, and shear modulus, $H_\infty \sim 9 \times 10^{10}$ Pa (see, e.g., Eq. (10)) as

$$\eta_0 = \frac{H_\infty}{\nu_0} \approx 10^{-1} \text{ Pa s}. \tag{15}$$

We demonstrated, in Ref. [21], that Avramov's jump frequency model for viscosity [22] and the Adam and Gibbs cooperative motion model [23] lead to similar results. Here, for its simplicity, we use the viscosity equation given in Ref. [22]

$$\eta = \eta_0 \exp\left(\varepsilon\left(\frac{T_g}{T}\right)^{\alpha'}\right). \tag{16}$$

Eq. (16) describes the viscosity, assuming that the building units jump with frequencies that depend on the particular activation energy they have to overcome (there is a distribution of activation energies due to the structural disorder in glasses). If we define T_g as the temperature at which the viscosity is $\lg \eta \approx 12.5$ Pa s, then the dimensionless parameter ε is given by

$$\varepsilon = 2.31 \times (12.5 - \lg \eta_0). \tag{17}$$

The *fragility parameter* α' [22] in Eq. (16) is proportional to the heat capacity of the melt. Typically, α' varies from 1 to 6 for multi-component silicate glasses and is 1 for pure SiO_2 glass. Low α' is typical for *long* glasses, while *short* glasses are characterized by high α' values.

There is a clear correlation between the reduced glass transition temperature and the crystallization pattern [24]. It can be shown (see also Table 1) that, when $T_g/T_m > 0.6$, only surface crystallization is observed in laboratory time scales, while internal crystallization is easily observed in glasses having $T_g/T_m < 0.6$.

We intend to elucidate the role of thermodynamic properties, such as $\Delta S_m/R$, in the behavior of crystallization. Therefore, it is important to verify whether the viscosity parameters, T_g or α', are related to this thermodynamic parameter. Despite the abundance of data on T_g and on α' (see e.g. [24,25]), there is only a limited amount of $\Delta S_m/R$ data [7,8,15,17,20], which is summarized in Table 1. We found no correlation between these kinetic and thermodynamic quantities.

A similar result, no correlation with $\Delta S_m/R$ (see Table 1), was obtained through a comparison of the parameters of the Vogel–Fulcher–Tamman (VFT) equation

$$\eta = \eta_0 \exp\left(\frac{B}{T - T_0}\right) \tag{18}$$

or the parameters of Adam and Gibbs

$$\eta = \eta_0 \exp\left(\frac{B^*}{T\Delta S}\right). \tag{19}$$

It could be argued that these kinetic parameters should be entropy sensitive because the configurational entropy, for instance, enters the denominator of the exponential term of the Adam and Gibbs equation (16). However, the kinetic parameters are quite insensitive to melting entropy because B^* is proportional to configurational entropy. The expressions

$$B = \varepsilon(T_g - T_0) \tag{20a}$$

and

$$B^* = \varepsilon T_g \Delta S_g \tag{20b}$$

relating B^* to the configurational entropy at the glass transition temperature, follow straightforwardly from Eq. (15) with the definition of $\eta(T_g)$ given there. The introduction of Eq. (20a) into Eq. (19) leads to

$$\eta = \eta_0 \exp\left(\varepsilon \frac{T_g}{T} \frac{1}{\left(1 + \frac{\Delta C_p}{\Delta S_g} \ln \frac{T}{T_g}\right)}\right) \approx \eta_0 \exp\left(\varepsilon\left(\frac{T_g}{T}\right)^{\alpha'}\right). \tag{21}$$

Table 1
Properties of several glass forming systems

Substance	$\eta = \eta_0 \exp\left(\varepsilon\left(\frac{T_g}{T}\right)^{\alpha'}\right)$			$\Delta S_m/R$	T_g/T_m	Mode of crystallization	$\eta = \eta_\infty \exp\left(\frac{B}{T-T_0}\right)$		
	$\lg \eta_0$ (Pa s)	T_g (K)	α'				$\lg \eta_\infty$ (Pa s)	B	T_0
SiO_2	1.6	1399	1.1	0.9	0.70	Surface			
$Li_2O \cdot 2SiO_2$	0.8	720	3.8	5.3	0.56	Bulk	0.73	1536	564
$2Li_2O \cdot 8SiO_2$	0.32		2.25						
$3Li_2O \cdot 7SiO_2$	0.53	708	3						
$Na_2O \cdot 3SiO_2$	1.48	761	4.25	4	0.7		−1.75	3216	530
$Na_2O \cdot 2SiO_2$	−0.2	692	2.5	4.7	0.59	Surface	−2.8	4774	381
$2Na_2O \cdot 8SiO_2$	−0.06	735	2.25						
$3Na_2O \cdot 7SiO_2$	−0.15	713	3		0.634		−1.49	2791	528
$4Na_2O \cdot 6SiO_2$	−0.15	678	2.5						
$44Na_2O \cdot 56SiO_2$	−0.42	669	3.25		0.51		−2.49	3132	453
$Na_2O \cdot SiO_2$	−1.9	673	2.8	2.3	0.5	Bulk	−4.7	4431	418
$2K_2O \cdot 8SiO_2$	0.84	751	2.5			Surface			
$BaO \cdot 2SiO_2$	−1.5	962	3.25	2.6	0.56	Bulk	−6.8	7822	554
$3PbO \cdot 7SiO_2$	0.66	743	3			Surface			
$4PbO \cdot 6SiO_2$	0.2	714	3.5			Surface			
$PbO \cdot SiO_2$	−0.04	655	4	7	0.63	Surface	−3	3008	456
$6PbO \cdot 4SiO_2$	−0.49	625	4.75			Surface			
$97.8B_2O_3 \cdot 2.17SiO_2$	1.38	520	3.25			Surface			
$94B_2O_3 \cdot 5.95SiO_2$	1.29	525	3			Surface			
$89.3B_2O_3 \cdot 10.7SiO_2$	1.45	527	3			Surface			
$51.6B_2O_3 \cdot 48.4SiO_2$	0.6	582	1.5			Surface			
$44.6B_2O_3 \cdot 55.4SiO_2$	−0.02	682	1			Surface			
B_2O_3	1.35	512	3.25	3.8	0.71	Surface	−0.4	2016	354.5
$13.5Na_2O \cdot 86.5B_2O_3$	0.09	637	3.5						
$33.3Na_2O \cdot 66.7B_2O_3$	−0.26	739	5.75						
$6Li_2O \cdot 94B_2O_3$	0.36	604	4.25						
$13.9Li_2O \cdot 86.1B_2O_3$	−0.19	676	4.75						
$33.5Li_2O \cdot 66.5B_2O_3$	−1.72	735	4.25			Bulk			
$19.5K_2O \cdot 80.5B_2O_3$	−0.16	675	4						
$24.4K_2O \cdot 75.6B_2O_3$	0	677	4			???			
$18BaO \cdot 82B_2O_3$	−0.97	790	4						
$23.9BaO \cdot 76B_2O_3$	−0.9	826	4.5						
$PbO \cdot 2B_2O_3$	0.09	780	9.5	15	0.74		−1.28	728	735
P_2O_5	−4.87	522	1	3.7	0.59	Surface	−4.87	9067	0
$Li_2O \cdot P_2O_5$	−0.79	580	5.5	8	0.63	Surface	−2.3	1141	509
$Na_2O \cdot P_2O_5$	0.43	544	5.5	3	0.61	Surface	−1	1095	466
GeO_2	1.34	923	1.4	1.3	0.67	Surface			
$5Na_2O \cdot 95GeO_2$	0.11	695	2.25						
$10Na_2O \cdot 90GeO_2$	−0.13	743	4.5						
$29.6Na_2O \cdot 70.4GeO_2$	0.43	710	6.5						
$20PbO \cdot 80GeO_2$	0.33	716	4.25						
$30PbO \cdot 70GeO_2$	0.66	679	6.25						
$40PbO \cdot 60GeO_2$	0.25	715	5						
$50PbO \cdot 50GeO_2$	0.33	626	5.25						
$20.96Na_2O \cdot 9CaO \cdot 70SiO_2$	0.22	775	2.83						
$Na_2O \cdot 2CaO \cdot 3SiO_2$	−2.57	821	2.77	6.8	0.53	Bulk	−5.3	5637	504
$CaO \cdot Al_2O_3 \cdot 2SiO_2$	−2.06	1105	3.5	8.9	0.60	??	−5.64	6535	745
$Na_2O \cdot Al_2O_3 \cdot 6SiO_2$	−8.58	1012	1	4.5	0.68	Surface			
$2Na_2O \cdot 1CaO \cdot 3SiO_2$	−5.54	742.3	3.2		0.513		−8.94	5376	485.6

The empirical observation that α' is not sensitive to melting entropy is explained by the fact that $\Delta C_p/\Delta S_g$ varies in quite a limited range.

3. Results

We introduce Eqs. (12), (13), and (16) into Eqs. (4) and (5), and integrate the latter numerically, a procedure similar to that used by Weinberg [11]. Our investigation is confined to the influence of three dimensionless parameters on q_{cr} (Eq. (5)) and K_H, and K_W (Eq. (1)): a thermodynamic parameter – reduced melting entropy, $\Delta S_m/R$, and two viscosity parameters – fragility α', and reduced glass transition temperature T_g/T_m.

It is not the purpose of this article to present results for particular compositions. Therefore, unless specified, computations are performed for a typical silicate glass, with $T_m = 1500$ K and $\eta_0 = 0.3$ (i.e. $\varepsilon = 30$ in Eq. (17)).

3.1. Homogeneous nucleation, $\Phi = 1$

Fig. 1(A) illustrates the overall crystallization rate calculated by introducing Eqs. (12)–(16) into Eq. (4) for a heating rate of $q = 0.01$ K/min. The value of $\Delta S_m/R$ is shown on each curve. Fig. 1(B) shows the derivatives of the curves of Fig. 1(A).

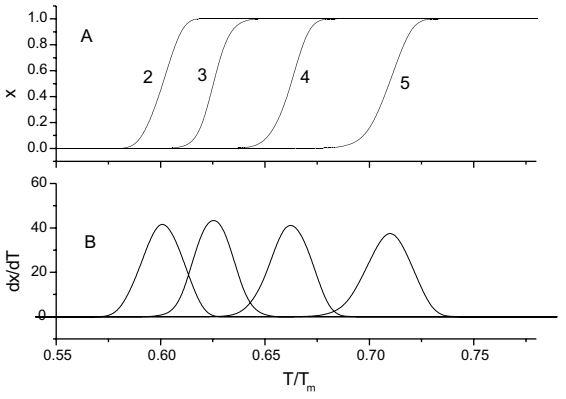

Fig. 1. (A) Overall crystallization rate for heating rate $q = 0.01$ K/min, $\Phi = 1$, $\alpha' = 3$, $T_g/T_m = 0.55$ and $\eta_0 = 0.3$. The curves were calculated by introducing Eqs. (12)–(16) into Eq. (4). The value of $\Delta S_m/R$ is shown on each curve. The corresponding temperature derivatives are shown in (B).

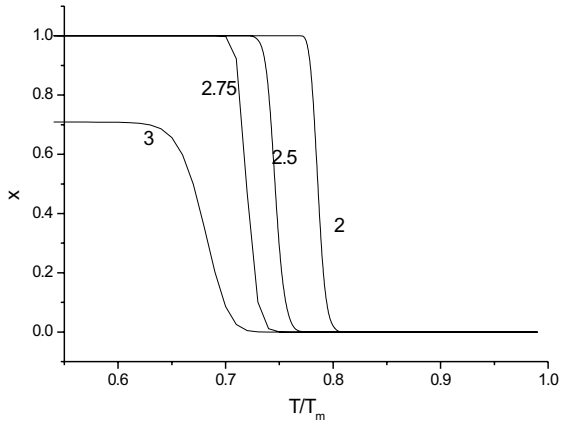

Fig. 2. Overall crystallization rate for cooling rate $q = 0.01$ K/min, $\Phi = 1$, $\alpha' = 3$, $T_g/T_m = 0.55$ and $\eta_0 = 0.3$. The value of $\Delta S_m/R$ is shown on each curve.

The maximum of each peak corresponds to the crystallization temperature, T_c^h (for instance, in a DSC experiment). It is interesting to note that high $\Delta S_m/R$ shifts the crystallization peak to higher temperatures.

Based on the same parameters used in Fig. 1, Fig. 2 shows that similar results are obtained upon cooling. It should be noted that the tendency to crystallize is much lower upon cooling than on reheating. For $\Delta S_m/R = 3$, for instance, the degree of crystallization achieved on cooling is incomplete while, on reheating, crystallization saturates at $T/T_m \sim 0.65$.

Fig. 3 shows that K_H and K_W, determined from T_c^h according to Eq. (1), increase with melting

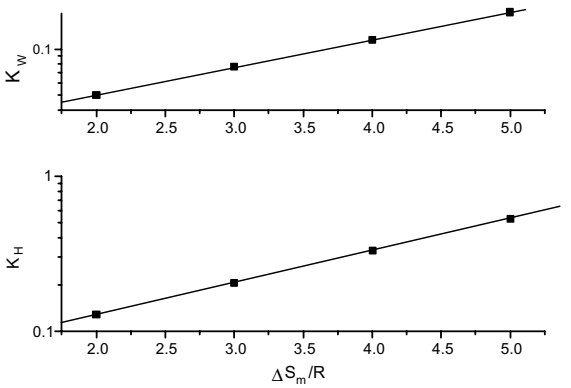

Fig. 3. K_H and K_W versus melting entropy.

entropy, according to the following (empirical) expressions:

$$\begin{cases} K_{\mathrm{H}} = 0.05 \times 10^{0.2\frac{\Delta S_{\mathrm{m}}}{R}}, \\ K_{\mathrm{W}} = 0.02 \times 10^{0.17\frac{\Delta S_{\mathrm{m}}}{R}}. \end{cases} \tag{22}$$

Fig. 4 shows the dependence of the critical cooling rate on melting entropy in log-lin coordinates. A relationship can be described as

$$\lg q_{\mathrm{cr}}(x_{\mathrm{c}}) = 1.35 - 0.25 \lg x_{\mathrm{c}} - 1.68 \frac{\Delta S_{\mathrm{m}}}{R}. \tag{23}$$

Analogous to the critical cooling rate one can formulate a critical heating rate $q_{\mathrm{cr}}^{(+)}$, defined as the lowest heating rate at which the sample can be heated from T_{g} to T_{m} so that crystallization will not exceed a certain x_{c}. The results shown in Fig. 4 demonstrate that the critical heating rate is much higher than the critical cooling rate and somewhat less sensitive to melting entropy. The resulting equation is

$$\lg q_{\mathrm{cr}}^{(+)}(x_{\mathrm{c}}) = 2.81 - 0.25 \lg x_{\mathrm{c}} - 1.17 \frac{\Delta S_{\mathrm{m}}}{R}. \tag{24}$$

Eqs. (20a)–(22) indicate that, for a given viscosity, in the absence of active nucleating centers, substances with higher melting entropy form glasses more readily and are more stable than those with low melting entropy, confirming the results of Uhlmann et al. [10].

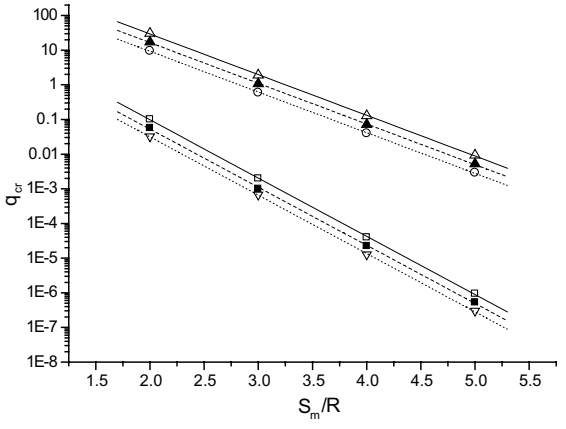

Fig. 4. Critical cooling rate q_{cr} and critical heating rate $q_{\mathrm{cr}}^{(+)}$ versus melting entropy. Critical cooling rate q_{cr}: (□) $x_{\mathrm{c}} = 10^{-4}$; (■) $x_{\mathrm{c}} = 10^{-3}$; (▽) $x_{\mathrm{c}} = 10^{-2}$. Critical heating rate $q_{\mathrm{cr}}^{(+)}$: (△) $x_{\mathrm{c}} = 10^{-4}$; (▲) $x_{\mathrm{c}} = 10^{-3}$; (○) $x_{\mathrm{c}} = 10^{-2}$.

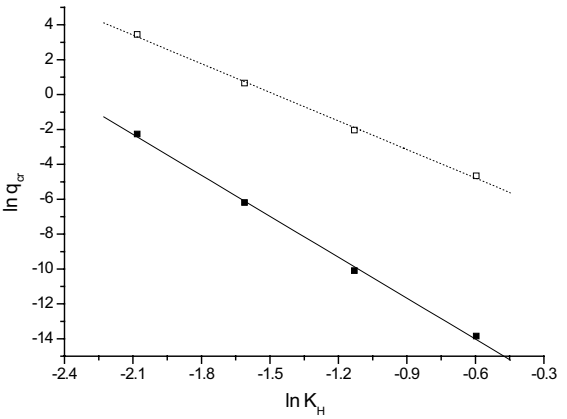

Fig. 5. Critical cooling rate q_{cr} (■) and critical heating rate $q_{\mathrm{cr}}^{(+)}$ (□) versus Hrubý parameter K_{H}.

Fig. 5 shows that the critical cooling rate q_{cr} decays with K_{H}. Substances with higher K_{H} are more stable on heating and are better glass formers on cooling from the melt. The following expressions result: $q_{\mathrm{cr}} K_{\mathrm{H}}^{5.5} = 0.0003$.

An analogous expression for the critical heating rate is $q_{\mathrm{cr}}^{(+)} K_{\mathrm{H}}^{7.8} = 7 \times 10^{-9}$.

Fig. 6 shows the dependence of the Hrubý parameter K_{H} and of critical cooling rate q_{cr} on the fragility α, in log-lin coordinates. Data for K_{H} are calculated for a heating rate of $q = 1$ K/min. K_{H} and q_{cr} change very rapidly with α', even in loga-

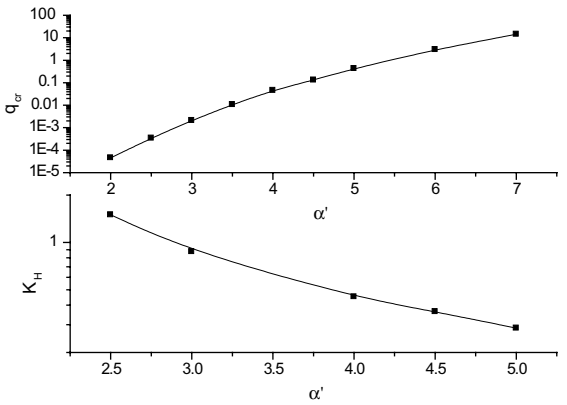

Fig. 6. Critical cooling rate, q_{cr}, and a Hrubý parameter, K_{H}, versus fragility α', in log-lin coordinates. Data for K_{H} are calculated for a heating rate of $q = 1$ K/min.

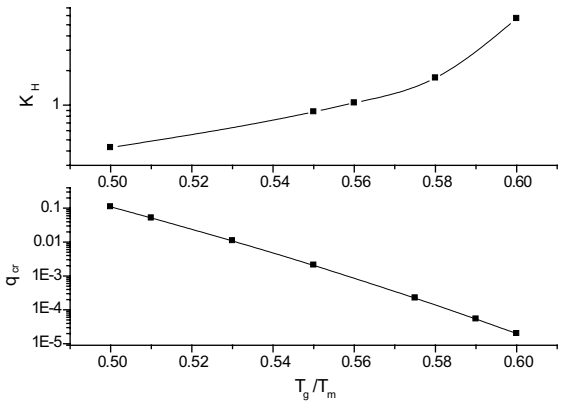

Fig. 7. Hrubÿ parameter K_H and critical cooling rate q_{cr} versus T_g/T_m, in log-lin coordinates. K_H results are calculated for heating rate $q = 1$ K/min.

rithmic coordinates. More fragile glasses crystallize easily, as we expected.

Fig. 7 shows the dependence of the Hrubÿ parameter K_H and of the critical cooling rate q_{cr} on T_g/T_m in log-lin coordinates. Again, data for K_H are calculated for a heating rate of $q = 1$ K/min. K_H and q_{cr} change very quickly with T_g/T_m, even in logarithmic coordinates. The higher the glass transition temperature, the easier it is to produce glasses on cooling and the more stable they are upon reheating.

3.2. Heterogeneous nucleation

Glass crystallization is usually determined by heterogeneous nucleation because it is difficult to avoid the presence of foreign solid particles. Moreover, in many cases, the sample surface can serve as a foreign substrate, thus provoking heterogeneous nucleation. For a first approximation, the heterogeneity parameter, $\Phi(< 1)$, depends on the surface energies, on the crystal/melt interfacial energy, $\sigma_{c/m}$, on the melt/vapor interfacial energy, $\sigma_{m/v}$, and on the crystal/vapor interfacial energy, $\sigma_{c/v}$, as

$$\Phi = \frac{1}{2}\left(1 - \frac{\sigma_{m/v} - \sigma_{c/v}}{\sigma_{c/m}}\right). \quad (25)$$

Hereinafter, the index c stands for crystal, the index m stands for a melt and the index v stands for vapor phase. The surface energies can be expressed similarly to Eq. (9) through the enthalpies of the corresponding phase transition. Thus, Eq. (25) transforms to

$$\Phi = \frac{1}{2}\left(1 - \frac{\alpha_{m/v}H_{ev} - \alpha_{c/v}H_{sub}}{\alpha_{c/m}H_m}\right). \quad (26)$$

Here α_{ij} denotes α for the corresponding interface. The sublimation enthalpy is equal, here, to the sum of evaporation enthalpy and melting enthalpy $H_{sub} = H_{ev} + H_m$. Therefore, when the three α_{ij} coefficients are equal, the wetting function determined by Eq. (26) becomes $\Phi = 1$, i.e., the surface is inactive (homogeneous nucleation). Conversely, when $\alpha_{c/m}$ is relatively large, $\Phi < 1$ and heterogeneous nucleation takes place at the sample's surface.

The dependencies of the critical cooling (and heating) rates on melting entropy change considerably in the case of heterogeneous nucleation. Even small *changes* of Φ exert a notable influence on q_{cr}. This is illustrated in Fig. 8, where the dependence of the critical cooling rate on melting entropy is compared for $\Phi = 1$ (squares) and $\Phi = 0.5$ (triangles). The curves are calculated according to Eq. (4), with $x_c = 10^{-4}$, $\alpha' = 3$, $T_g/T_m = 0.55$ and $\lg \eta_0 = 0.3$. It should be noted that, in these calculations of heterogeneous nucleation, the computed nucleation rate was overestimated because the number of active centers was assumed to be equal to the number of molecules of the system

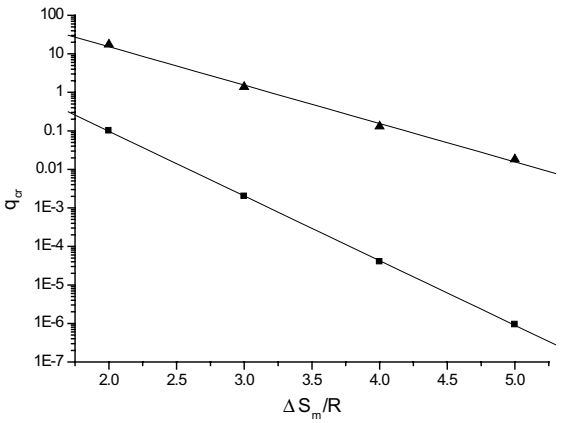

Fig. 8. Critical cooling rate q_{cr} versus melting entropy for $\Phi = 0.01$ and $\alpha_s = 0.3$; $x_c = 10^{-4}$, $\alpha' = 3$, $T_g/T_m = 0.55$, and $\lg \eta_0 = 0.3$.

(this is true in homogeneous nucleation). In other words, it involves at least two additional assumptions: (i) there is an extremely large concentration of active centers, and (ii) although the nucleation rate is increased, it is still sufficiently low so that the number of nuclei remains much lower than the number of active substrates. The other extreme case (and often more realistic) is to assume that there are N (*per unit volume*) active centers whose nucleation is infinitely fast. In this case, Eq. (4) should be replaced by

$$x(q) = 1 - \exp\left\{ -\frac{4\pi}{3q} \int_{T_m}^{T} J(T', \Phi = 1) \times \left[\frac{1}{q} \int_{T'}^{T} G(T'')\,\mathrm{d}T'' \right]^3 \mathrm{d}T' - \frac{4\pi}{3} N \left[\frac{1}{q} \int_{T_m}^{T} G(T'')\,\mathrm{d}T'' \right]^3 \right\}. \quad (27)$$

For large N, the critical cooling rate determined from Eq. (27) is

$$q_{cr}(x_c) = \int_{T_m}^{T_g} G(T'')\,\mathrm{d}T'' \left[-\frac{\frac{4\pi}{3}N}{\ln(1 - x_c)} \right]^{\frac{1}{3}}. \quad (28)$$

The change, in this case, is much more significant for cooling runs than for heating experiments. Upon heating, the maximum nucleation rate temperature is attained first; therefore, the samples reach the maximum growth rate interval having a relatively large number of nuclei, regardless of N. On the other hand, on cooling, the maximal growth rate interval is reached with only N nuclei. It should be noted that similar considerations are valid for the case of homogeneous nucleation. That is why critical heating rates are always higher than critical cooling rates.

Fig. 9 shows the dependence of the Hrubÿ parameter on the number N of active centers. Data are computed for $\Delta S_m/R = 3$. In the region of low N (compared to the number of nuclei formed during heating through the region of maximal nucleation), N is unimportant in the overall crystallization process.

Fig. 10 shows the dependence of the critical cooling rate q_{cr} on $\Delta S_m/R$ for a number of $\lg N$ values given at each curve; q_{cr} increases with melting entropy. The reason is that overall crystallization, in this case, is controlled by the linear growth rate and not by the nucleation rate.

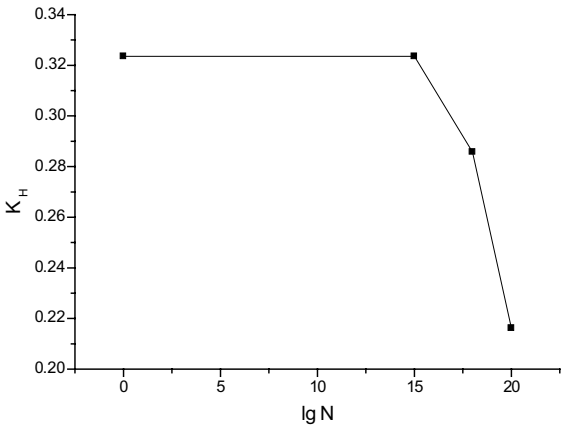

Fig. 9. Hrubÿ parameter K_H versus N, in lin-log coordinates. The points are calculated for $\alpha' = 3$, $T_g/T_m = 0.55$, $\eta_0 = 0.3$ and $\Delta S_m/R = 3$.

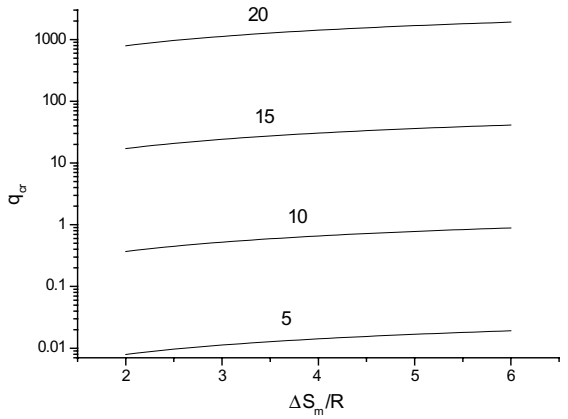

Fig. 10. Critical cooling rate q_{cr} versus $\Delta S_m/R$ for several $\lg N$ given at each curve.

4. Discussion

In the case of homogeneous crystallization, the tested stability parameters K_H and K_W increase (indicating great stability on heating), while the critical cooling rates decrease with melting entropy. Thus, the tendency to crystallize decreases as $\Delta S_m/R$ increases. The situation is quite different in the case of heterogeneous nucleation (see

Fig. 10). The negative slope of $q_{cr}(\Delta S_m/R)$ dependence is due to the increase of the linear growth rate with melting entropy (Fig. 4).

It is interesting to note that, for a given set of parameters, the critical cooling rate is several orders of magnitude lower than the corresponding critical heating rate. Samples that vitrify at a given cooling rate could crystallize completely if heated at the same heating rate. The reason is that, as it cools, the melt first crosses the region of high growth rate with a small number of nuclei, while, on heating, the nuclei first cross the high nucleation rate region. This effect is accounted for by the double integral given in Eqs. (2) and (4). This integral is often replaced by a product of two integrals. In the case of isothermal crystallization, this procedure does not lead to important errors. However, such a procedure is inadmissible for non-isothermal treatment with simultaneous nucleation and growth, as shown by Weinberg and Zanotto [8].

Figs. 6 and 7 confirm that the more *fragile* glass-forming substances easily crystallize, as one expects. In other words, *long glasses* are more stable than *short glasses*. However, the direct correlation between GFA and GS that is demonstrated in the present work was not found in Ref. [11].

We believe that the assumption in Ref. [11] that changes in B (with constant T_0) must be accompanied by equivalent changes in η_0 (T_g remains constant, determining that a glass with larger activation energy B has a lower viscosity) explains the discrepancy between the results of Ref. [11] and the present findings.

Let us consider two glasses. Their activation energies (B and B') and pre-exponentials (η_0 and η_0') are different, although T_0 and T_g are the same for both of them. Thus, the VFT equations for these glasses are

$$\eta = \eta_0 e^{\frac{B}{T-T_0}} \quad \text{and} \quad \eta' = \eta_0' e^{\frac{B'}{T-T_0}} \tag{29}$$

and the condition of constant viscosity at T_g gives $\eta_0' = \eta_0 e^{(B-B'/T_g-T_0)}$. One can easily obtain the following expression for η'/η ratio:

$$\frac{\eta'}{\eta} = e^{(B'-B)\frac{T_g-T}{(T_g-T_0)(T-T_0)}}. \tag{30}$$

It follows that, above the glass transition temperature, $\eta' < \eta$, for $B' < B$. In other words, an increase in the activation energy causes a decrease in viscosity. This particular situation is responsible for an apparent increase in the critical cooling rate in Ref. [11]. Moreover, Fig. 12 shows that $(T_g - T_0)/T_m$ is not a perfect constant, as assumed in Ref. [11]. A summary of existing experimental data indicates that $T_g - T_0/T_m \approx 0.38 - 0.5(T_0/T_m)$.

Our finding that GFA and GS are directly proportional agrees with the results of Cabral et al. [12], who have experimentally tested the Hrubÿ parameter vs. q_{cr} for a set of four selected glasses that undergo homogeneous nucleation. Cabral et al. [25] recently extended their test to seven glasses and confirmed the results of Ref. [12].

4.1. Limitations of the approach

Fig. 11 shows the temperature dependencies of the nucleation rate J and of the linear growth rate G of $Li_2O \cdot 2SiO_2$ glass using data reported in [20,26]. Lines are computed according to Eqs. 12,13 for $\alpha = 0.389$ and values of the parameters for this composition, listed in Table 1. The fit is far from perfect, especially for the nucleation rate, but there are several possible error sources.

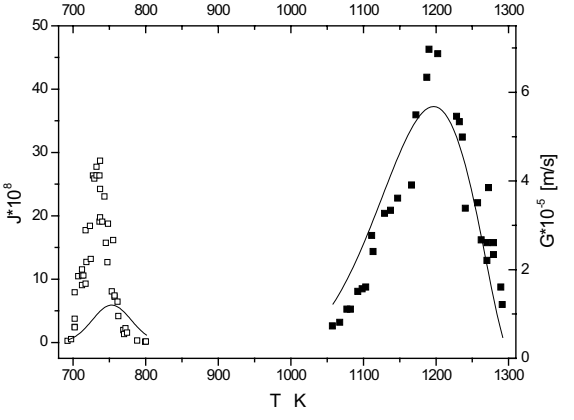

Fig. 11. Calculated temperature dependencies of the nucleation rate J and linear growth rate G in $Li_2O \cdot 2SiO_2$ glass. Experimental data are from Refs. [20,26]. Lines are computed according to Eqs. 12,13 for $\alpha = 0.389$ and the values of the parameters for this composition listed in Table 1.

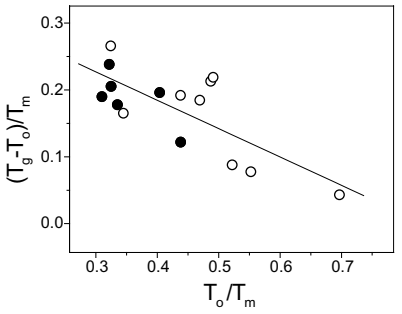

Fig. 12. Available data for $(T_g - T_0)/T_m$ versus T_0/T_m for 15 glasses. See Table 1. Solid symbols correspond to glasses that display homogeneous nucleation. $(T_g - T_0)/T_m$ vary from 0.05 to almost 0.3.

Among these lies the classic assumption of capillarity of the classic nucleation theory, which is limited to rather large nuclei with sharp interfaces. At high supersaturation, however, the nuclei/glass interfaces may be quite diffuse. Since there are no independent measurements of surface tension, σ, and any model specifying these dependencies is rather unreliable, for the sake of simplicity we have assumed that σ is temperature and size independent.

Despite these limitations, the present non-isothermal treatment (continuous cooling or heating) is more accurate than the classic TTT-treatment. The main purpose of this investigation: to monitor the trends of crystallization with certain parameters and to test the possible correlation between GFA and GS, has thus been achieved.

5. Conclusions

The approach used here enabled us to evaluate the effect of both homogeneous and heterogeneous crystallization on GS and GFA.

GFA and GS follow the same trend with the three parameters tested here. Namely, when K_H and K_W increase, indicating an increase in GS, the critical cooling rate decreases, showing an increase of GFA. We thus demonstrated that GFA and GS are directly related.

Acknowledgements

The authors gratefully acknowledge the critical comments of Vladimir Fokin. The financial support of CNPq, Pronex and Fapesp (Brazil) is fully appreciated.

References

[1] V. Goldschmidt, Skrifter Norske Videnskaps. Akad. (Oslo) I, Matematisch-Naturwiss. Klasse 1 (1926) 7.
[2] W. Zachariasen, J. Am. Chem. Soc. 54 (1932) 3841.
[3] G. Tamman, Die Aggregatzustaende, Leopold Voss, Leipzig, 1922.
[4] A. Dietzel, H. Wiekert, Glastech. Ber. 29 (1956) 1.
[5] D. Turnbull, M. Cohen, in: Mackenzie (Ed.), Modern Aspects of Vitreous State, 1960, p. 38.
[6] I. Gutzow, J. Schmelzer, The Vitreous State, Springer, 1995.
[7] D.R. Uhlmann, J. Non-Cryst. Solids 7 (1972) 337.
[8] M.C. Weinberg, E.D. Zanotto, Phys. Chem. Glasses 30 (1989) 110.
[9] M.C. Weinberg, D.R. Uhlmann, E.D. Zanotto, J. Am. Ceram. Soc. 72 (1989) 2054.
[10] D.R. Uhlmann, B.J.J. Zelinski, E.D. Zanotto, M.C. Weinberg, Sensitivity of critical cooling rate to model and material parameters, Proceedings of the XV International Congress on Glass, Leningrad, USSR, July, 1989, vol. 1A, p. 156.
[11] M.C. Weinberg, J. Non-Cryst. Solids 167 (1994) 81.
[12] A.A. Cabral Jr., C. Fredericci, E.D. Zanotto, J. Non-Cryst. Solids 219 (1997) 182.
[13] A. Kolmogorov, Izv. Acad. Sci. USSR, Ser. Math. 1 (1937) 355.
[14] M. Avrami, J. Chem. Phys. 7 (1939) 1103.
[15] M. Avrami, J. Chem. Phys. 8 (1940) 212.
[16] G. Voelksch, private communication, Jena, 2001.
[17] V.M. Fokin, O. Potapov, E.D. Zanotto, J. Non-Cryst. Solids, submitted for publication (2003).
[18] M.C. Weinberg, S. Manrich, E.D. Zanotto, Phys. Chem. Glasses 33 (1992) 99.
[19] I. Avramov, I. Gutzow, E. Grantscharowa, J. Cryst. Growth 87 (1988) 305.
[20] N. Diaz-Mora, E.D. Zanotto, V.M. Fokin, Phys. Chem. Glasses 39 (1998) 91.
[21] I. Avramov, J. Schmeltzer, E.D. Zanotto, in preparation.
[22] I. Avramov, J. Non-Cryst. Solids 262 (2000) 258.
[23] G. Adam, J. Gibbs, J. Chem. Phys. 43 (1963) 139.
[24] E.D. Zanotto, J. Non-Cryst. Solids 89 (1987) 361.
[25] A.A. Cabral, A.A.D. Cardoso, E.D. Zanotto, this issue, p. 1.
[26] O. Mazurin, M. Streltsina, T. Shvaiko-Shvaikovskaya, Handbook of Glass Data, Elsevier, Amsterdam, 1985.